Clinica Chimica Acta 492 (2019) 102–113

Contents lists available at ScienceDirect

Clinica Chimica Acta

journal homepage: www.elsevier.com/locate/cca

Relative quantification of plasma N-glycans in type II congenital disorder of glycosylation patients by mass spectrometry

E.A. Barbosa[a,b], N. do C. Fontes[c], S.C.L. Santos[d], D.J. Lefeber[e], C. Bloch[b], J.M. Brum[c], G.D. Brand[a,*]

[a] Laboratório de Síntese e Análise de Biomoléculas - LSAB, Instituto de Química – IQ, Universidade de Brasília – UnB, Brasília, DF, Brazil
[b] Laboratório de Espectrometria de Massa – LEM, Embrapa Recursos Genéticos e Biotecnologia, Brasília, DF, Brazil
[c] Laboratório de Genética Bioquímica, Rede Sarah de Hospitais de Reabilitação, Brasília, DF, Brazil
[d] Laboratório de Biologia Molecular, Rede Sarah de Hospitais de Reabilitação, Brasília, DF, Brazil
[e] Department of Neurology, Translational Metabolic Laboratory, Donders Center for Brain, Cognition, and Behavior, Radboud University Medical Center, Nijmegen, the Netherlands

ARTICLE INFO

Keywords:
Mass spectrometry
Glycomics
Clinical chemistry
Congenital disorders of glycosylation
LC–MS
Inborn errors of metabolism

ABSTRACT

Background: Type II Congenital Disorders of Glycosylation (CDG-II) are a group of diseases with challenging diagnostics characterized by defects in the processing of glycans in the Golgi apparatus. Mass Spectrometry (MS) has been a valuable tool in the definition of CDG-II subtypes. While some CDG-II subtypes are associated with specific N-glycan structures, others only produce changes in relative levels, reinforcing the demand for quantification methods.

Methods: Plasma samples from control individuals were pooled, derivatized with deuterated iodomethane (I-CD_3), and used as internal standards for controls and patients whose glycans were derivatized with iodomethane (I-CH_3), followed by MALDI MS, LC–MS and -MS/MS analyses.

Results: Total N-glycans from fifteen CDG-II patients were evaluated, and 4 cases with molecular diagnosis were considered in detail: 2ATP6V0A2-CDG siblings, and 2 MAN1B1-CDG patients, one of them carrying a previously undescribed p.Gly536Val mutation.

Conclusions: Our methodology offers a feasible alternative to the current methods for CDG-II diagnosis by MS, which quantify glycan structures as fractions of the total summed signal across a mass spectrum, a strategy that lowers the variability of minor components. Moreover, given its sensitivity for less concentrated yet biologically relevant structures, it might assist the uncovering of novel diagnostic glycans in other CDG-II subtypes.

1. Introduction

Anomalous glycosylation profiles are observed in a range of pathological conditions [1] and tend to be the product of structural and functional alterations in the enzymes and/or organelles involved in the synthesis and in the processing of glycoconjugates [2]. Congenital disorders of glycosylation (CDG) comprise > 130 disorders involving genetic defects of glycosylation, with approximately 60% affecting N-glycosylation pathways [3,4]. CDGs can impair the functioning of several organs, leading to diverse clinical presentations, such as ataxia, coagulopathies, liver disease, retinopathy, dysmorphic features and hypotonia [5]. N-glycosylation disorders are organized in two major groups: CDG-I, characterized by defects in the synthesis of lipid-linked oligosaccharides and its transfer to the emerging polypeptide chains in the endoplasmic reticulum (ER); and CDG-II, which result from defects in the trimming/processing reactions of glycans in the Golgi apparatus [2,3]. Whereas CDG-I can be satisfactorily detected by routine Isoelectric Focusing (IEF) of transferrin in plasma [6], screening CDG-II can be more challenging, demanding a complementary approach, provided mostly by Mass Spectrometry (MS) [3,6–8]. In cases where MS is insufficient [3], DNA sequencing might be needed for accurate diagnostics. The subtyping of CDG is even more relevant now that it has been demonstrated that dietary intervention results in clinical improvement for some subtypes [9].

Mass Spectrometry is an important tool in the definition of CDG-II subtypes. Direct mass analysis of intact transferrin or free plasma N-glycans using either MALDI MS or Q-ToF Mass Spectrometry provides diagnostic profiles for some subtypes, such as MGAT2-CDG, B4GALT1-

* Corresponding author.
E-mail address: gdbrand@unb.br (G.D. Brand).

https://doi.org/10.1016/j.cca.2019.02.013
Received 5 November 2018; Received in revised form 12 February 2019; Accepted 13 February 2019
Available online 15 February 2019
0009-8981/

CDG, SLC35A1-CDG, SLC35A2-CDG, PGM1-CDG and MAN1B1-CDG [8,10]. Also, a differential N-tetrassacharide has been demonstrated in ALG1- CDG, PMM2- CDG or MPI-CDG [11], while three novel glycan structures were associated with MAN1B1-CDG [12,13]. However, CDG-II subtypes such as COGx-CDG [6,7,14–16], TMEM165-CDG [17], and the V-ATPase defects [18–21], produce only quantitative changes in serum N-glycans, creating a demand for reliable methods of quantification [8]. Recently, relative and absolute quantitative glycomics methodologies have been developed [22,23,24]. Relative quantification of glycans can be performed by the calculation of peak areas in a MALDI spectrum using a standard [7], or alternatively by analyzing paired samples using a stable isotope labelling (SIL) strategy [25,26]. The most popular SIL strategy concerns the use of light (I-CH_3) and heavy (I-CD_3, I-$^{13}CH_3$ or I-$^{12}CDH_2$) isotopes in the permethylation of glycans, a strategy that allows the concomitant detection of both negatively charged and neutral glycans in a single acquisition. By this technique, the ratios of light and heavy isotopes are used to measure relative changes in glycan abundance, using a control as reference.

The present work uses a SIL strategy coupled to mass spectrometry analysis to quantify plasma N-glycans of CDG-II patients in relation to a cohort of control individuals. Plasma samples of control individuals were pooled and permethylated with a heavy iodomethane isotope (I-CD_3), mixed with individual patient samples derivatized with non-deuterated iodomethane (I-CH_3), and submitted to MALDI MS and LC–MS. The assignment of glycan structures to the detected ions was performed by MS/MS analysis. The relative quantification of N-glycans was performed using the same or the most structurally similar heavy isotope available, in a "nearest neighbor" approach [27]. Therefore, the present methodology differs from previous mass spectrometric evaluations of CDG-II patients, which describe glycan structures as a percentage of the total summed signal across a mass spectrum, a strategy that lowers the variability of minor components and that may result in inaccurate relative quantification of biologically relevant molecular species [6,7]. Thirty-five ions from various N-glycan structures were quantified by MALDI MS, while LC–MS allowed the analysis of 86 ions. A statistical assessment of the distribution of glycans in normal individuals using a glycan-by-glycan approach was conducted, and fifteen putative CDG-II patients diagnosed by abnormal transferrin isoelectric focusing (IEF) profile and/or laboratory tests were evaluated. Two ATP6V0A2-CDG patients with molecular diagnosis were considered in detail, as well as one previously diagnosed MAN1B1-CDG patient and another individual with MAN1B1-CDG-compatible plasma glycan profile, bearing a homozygous novel mutation. Clinical and biochemical evaluation of the remaining eleven CDG-II patients is being conducted and will result in a complementary publication.

2. Material and methods

2.1. Reagents

MALDI-TOF Calibrant mixture (Calibration Standard II) and 2,5-dihidroxibenzoic acid (DHB) were from Bruker Daltonics. APCI positive calibration solution was from AB Sciex. Centricon (10-kDa cutoff) was purchased from Millipore. Iodomethane (I-CH_3), deuterated iodomethane (I-CD_3), dimethyl sulfoxide, sodium hydroxide, sodium acetate, iodoacetamide, dithiothreitol (DTT), ammonium carbonate, guanidine chloride, trypsin and PNGase F were obtained from Sigma–Aldrich. Sep-Pak SPE Strata C_{18} cartridges were from Phenomenex. All other reagents were of spectrometry or chromatography grade.

2.2. Samples

Blood plasma of 15 putative CDG-II patients, diagnosed by transferrin isoelectric focusing (IEF) and genetic sequencing, aged between 1 and 13 y, were comprehended in this study, including a previously diagnosed a MAN1B1-CDG patient [12]. Control plasma was obtained from 43 normal patients, aged between 1 and 13 y, all referred to Rede Sarah de Hospitais with symptoms and laboratory tests not compatible with CDG, and additionally a normal pattern of glycosylation as determined by transferrin IEF. Informed consent was obtained from patients and controls, or their legal guardians, and the study was approved by the Rede Sarah de Hospitais Ethics Committee. All experiments were performed in accordance with relevant guidelines and regulations.

2.3. N-glycans isolation and permethylation

Isolation of N-linked oligosaccharides was performed as previously described, with minor modifications [28]. Briefly, 40 µl of serum plasma were submitted to PNGase F digestion after protein reduction, alkylation, filtration through size-exclusion Centricon with 10-kDa cutoff (15 mins and 14.000 rpm), and trypsin digestion. The resulting free N-glycans were purified using a Sep-Pak C_{18} column eluting with 5% acetic acid. For permethylation, freeze dried samples were dissolved in DMSO saturated with freshly prepared NaOH. Iodomethane (I-CH_3) or deuterated iodomethane (I-CD_3) was added to the solution under a stream of nitrogen followed by sonication. The permethylation reaction was stopped by addition of 5% acid acetic in ice bath. Permethylated N-glycans were extracted using chloroform, washed twice with water, and dried under a stream of nitrogen. For purification, samples were dissolved in methanol, applied in a Sep-Pak C_{18} column (previously equilibrated with water) and washed with 10% acetonitrile. Permethylated N-glycans were eluted with 80% acetonitrile, and then freeze dried.

2.4. Determination of N-glycan profile from blood serum of normal and CDG-II patients

The blood plasma of control patients (43 samples) was joined in a solution denominated control pool. N-glycans from the control pool were permethylated using deuterated iodomethane (I-CD_3, heavy glycans), while plasma N-glycans each control and CDG-II patients were independently permethylated using regular iodomethane (I-CH_3, light glycans). Solutions containing light- and heavy-derivatized N-glycans were joined in a proportion of 2:1 (*v*/v) and jointly submitted to the final step of SPE purification, via Sep-Pak C_{18} column. The resulting 43 controls and 3 CDG-II patients light/heavy glycan mixtures were analyzed by MALDI-MS, LC–MS, and LC–MS/MS. The ratio between signals produced in mass spectra or TIC (for MALDI- and LC–MS, respectively) by light and the correspondingly heavy N-glycan was calculated (I-CH3/I-CD3 signals). Choice of the heavy reference for glycan structure quantification was based on both structural similarity and signal intensity (Table 1). Masses of N-glycan structures (permethylated and perdeuterated) were calculated using Glycoworkbench 2.0 software [29].

2.5. Mass spectrometry acquisitions and analysis

2.5.1. MALDI MS

Samples were dissolved in 30 µl of acetonitrile, mixed with 2,5-dihidroxybenzoic acid (DHB) ionization matrix (10 mg/ml in acetone containing sodium acetate 3 mmol/l) in a proportion of 1:3 and spotted on a MALDI-target plate. Acquisitions were performed using a UltraFlex Xtreme mass spectrometer (Bruker Daltonics) operating in the positive mode, controlled by FlexControl 4.0 software. The mass range analyzed was between *m/z* 1500–4500. Mass spectrometer was calibrated using Peptide Calibration Standard II. Mass spectra analysis as well as calculation of the areas under peaks produced by ionization of derivatized N-glycans (permethylated and perdeuterated) were performed using FlexAnalysis 3.4 software. Spectra were re-calibrated using ions *m/z* 1835.9, 2431.2, 3211.6, 4052.0, and 4413.2 as internal standards. Mass

Table 1
N-glycan number, structure, accurate mass ($[M + Na]^+$), mass used for quantitation, corresponding adduct, and the heavy reference glycan number used for LC–MS and MALDI MS quantification methods. Additionally, structural confirmation based on MS/MS spectra is indicated when available (Supplemental material 2 and 3).

Number	Proposed structure, theoretical mass and composition	Mass used for quantitation	Adduct	Heavy reference		Structure confirmed by MS/MS data[a]
				LC-MS	MALDI	
5	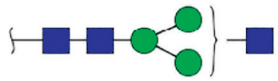 m/z: 1416.7094 [MONO,perMe,Na,0,freeEnd] HexNAc3Hex3	1416.7094	$[M+Na]^+$	3	-	
13	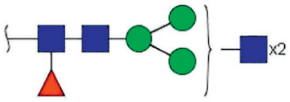 m/z: 1835.9249 [MCNO,perMe,Na,0,freeEnd] HexNAc5Hex3Fuc1	929.4571	$[M+2Na]^{2+}$	13	13	✓✓
14	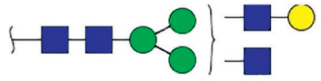 m/z: 1865.9355 [MONO,perMe,Na,0,freeEnd] HexNAc4Hex4	1865.9355	$[M+Na]^+$	19	-	
15	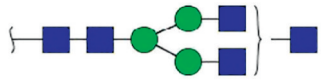 m/z: 1906.9620 [MONO,perMe,Na,0,freeEnd] HexNAc5Hex3	964.9756	$[M+2Na]^{2+}$	13	-	
19	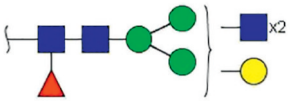 m/z: 2040.0247 [MCNO,perMe,Na,0,freeEnd] HexNAc4Hex4Fuc1	1031.5070	$[M+2Na]^{2+}$	19	19	✓✓
20	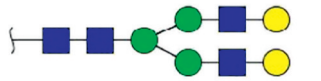 m/z: 2070.0352 [MONO,perMe,Na,0,freeEnd] HexNAc4Hex5	1046.5122	$[M+2Na]^{2+}$	20	27	✓✓
21	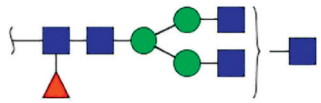 m/z: 2081.0512 [MCNO,perMe,Na,0,freeEnd] HexNAc5Hex3Fuc1	1052.0202	$[M+2Na]^{2+}$	13	13	

(*continued on next page*)

Table 1 (*continued*)

24	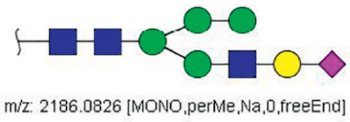 m/z: 2186.0826 [MONO,perMe,Na,0,freeEnd] HexNAc3Hex5NeuAc1	1104.5359*	$[M+2Na]^{2+}$	24	35	✓✓
26	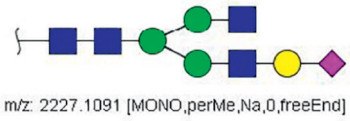 m/z: 2227.1091 [MONO,perMe,Na,0,freeEnd] HexNAc4Hex4NeuAc1	1125.0492	$[M+2Na]^{2+}$	26	35	✓✓
27	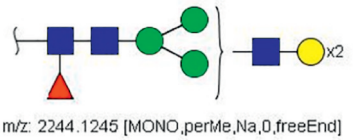 m/z: 2244.1245 [MONO,perMe,Na,0,freeEnd] HexNAc3Hex5Fuc1	1133.5568	$[M+2Na]^{2+}$	27	27	✓✓
28	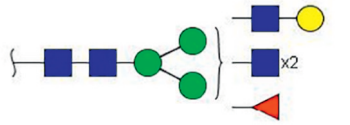 m/z: 2285.1510 [MONO,perMe,Na,0,freeEnd] HexNAc5Hex4Fuc1	1154.0701	$[M+2Na]^{2+}$	19	19	✓
31	 m/z: 2360.1718 [MCNO,perMe,Na,0,freeEnd] HexNAc3Hex5Fuc1NeuAc1	1191.5805	$[M+2Na]^{2+}$	58	-	
32	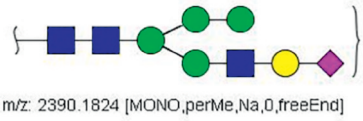 m/z: 2390.1824 [MONO,perMe,Na,0,freeEnd] HexNAc3Hex6NeuAc1	1206.5858	$[M+2Na]^{2+}$	32	35	✓✓
34	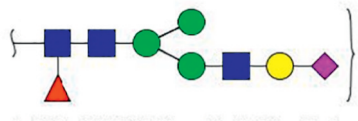 m/z: 2401.1983 [MONO,perMe,Na,0,freeEnd] HexNAc4Hex74Fuc1NeuAc1	1220.0808	$[M+Na+K]^{2+}$	34	-	✓✓
35	 m/z: 2431.2089 [MONO,perMe,Na,0,freeEnd] HexNAc4Hex5NeuAc1	1227.0991	$[M+2Na]^{2+}$	35	35	✓✓

(*continued on next page*)

Table 1 (*continued*)

40	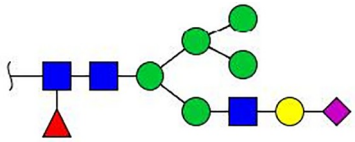 m/z: 2564.2716 [MCNO,perMe,Na,0,freeEnd] HexNAc3Hex6Fuc1NeuAc1	1293.6304*	$[M+2Na]^{2+}$	58	-	
52	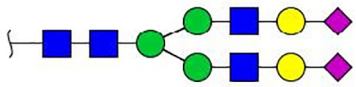 m/z: 2792.3826 [MONO,perMe,Na,0,freeEnd] HexNAc4Hex5NeuAc2	1407.6859	$[M+2Na]^{2+}$	52	52	✓✓
80	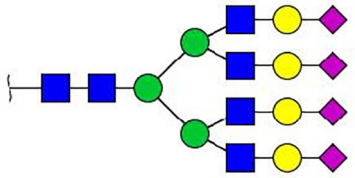 m/z: 4413.182[illegible] [MONO,perMe,Na,0,freeEnd] HexNAc6Hex7NeuAc4	1120.5374	$[M+4Na]^{4+}$	80	52	✓✓

Legend: ■ N-acetyl glucosamine (GlcNac), ● Mannose (Man), ● Galactose (Gal), ◀ Fucose (Fuc), ♦ Sialic acid (NeuAc).

lists were generated applying Snap Peak Detection Algorithm, TopHat Baseline Subtraction and Signal to Noise Threshold equal to 6. Values obtained were exported to Microsoft Excel for further calculations and statistical analyses.

2.5.2. LC–MS

Samples were dissolved in 40 µl MeOH containing 10 mmol/l sodium acetate. For mass spectrometry acquisitions, 6 µl were automatically injected by a ekspert^{tm}ultraLC 100-XL chromatography system (Eksigent) coupled to a Kinetex 2.6 µm C_{18} 100 Å (50 × 2.1 mm) LC Column connected to a TripleTOF 5600+ mass spectrometer (Sciex) housing a DuoSpray Ion Source. Reverse phase chromatography was performed using Milli-Q H_2O containing formic acid 0.1% (solvent A) and MeOH containing formic acid 0.1% (solvent B). Samples eluted across a linear gradient of solvent B ranging from 30 to 95% with a flow rate of 0.2 ml/min in 10 min. During analysis, chromatographic column was maintained at a constant temperature of 40 °C. Ion source operated in the positive mode at a temperature of 650.0 °C. Mass spectrometer worked in the High-Resolution mode with curtain gas equal 15. The mass rage of acquisitions was between *m/z* 800–2000. The other acquiring parameter were: number of cycles = 2043; polarity = positive; period cycle time = 525 ms; pulser frequency = 13.569 kHz and accumulation time = 500.00 ms. Mass spectrometer was calibrated using APCI positive calibration solution before acquisitions. Quantification of peak areas was performed using MultiQuant^{tm} 3.0.2 software (Sciex). LC–MS acquisitions were re-calibrated using peaks *m/z* 946.1203, 1220.0808, 1407.6859, 1466.5531, 1579.7826, 1649.2157, 1783.8824, 1812.8858, and 1888.3565 as internal standards. Ions were extracted using theoretical glycan masses ± 0.005 Da. Area values were exported to Excel for further calculations and statistical analyses.

MS/MS spectra of N-glycans were acquired in IDA (Information Dependent Acquisition) mode. Ions from charge state 2 to 4 were selected for fragmentation using dynamic collision energy mode. LC–MS/MS data were converted from WIFF to mzXML format using MSConvert (ProteoWizard 3.0) and fragmentation spectra were automatically annotated using GRITS Toolbox 1.2 software. The parameters of annotation were: 5.0 ppm of accuracy MS; 500 ppm of accuracy MSn; 5.0% of fragment intensity cut-off; perMe or perDMe derivatization type; free reducing end; N-glycans – 1190 glycans search data base; maximum of 3 cleavages; maximum of 1 cross ring cleavages; glycosidic cleavages of B, Y, C and Z series; cross ring cleavages of A and X series; maximum of 4 charges as Sodium adducts. The annotated spectra were exported to Excel and printed to PDF files. Additionally, some spectra whose precursor ion mass matched accurately to N-glycans that were not annotated by GRITS Toolbox were analyzed and annotated using GlycoWorkbench 2.1 build 146 software.

2.6. Genotyping and mutation analysis

Genomic DNA was extracted from peripheral blood samples according to a standard protocol. The codifying and flanking regions of all exons of MAN1B1 and ATP6V0A2 genes were amplified by PCR. Primer sequences were designed by Primer Blast Designing Tool (http://www.ncbi.nlm.nih.gov/tools/primer-blast) (Supplemental material 4). Both primer sequences and PCR conditions are available under request. Direct sequencing by Sanger method was performed in both directions (Big Dye Terminator Cycle Sequence kit v.3.0 and ABI3130 automated Sequencer, Applied Biosystems). The reference MAN1B1 and ATP6V0A2 sequences were obtained from GeneBank with accession numbers NM_012463, NP_036595.2, NM_016219.4, and NP_057303.2,

respectively. Mutation numbering is based on cDNA CCDS7029.1 and CCDS9254.1, respectively. The pathogenic role of novel missense mutations that were neither found in Clinvar (https://www.ncbi.nlm.nih.gov/clinvar/) nor HGMD professional (https://portal.biobase-international.com/hgmd/pro/) or ExAC or 1000Genomes (https://www.ncbi.nlm.nih.gov/variation/tools/reporter) were evaluated by testing three in silico on line tools: PolyPhen-2 (Polymorphism Phenotyping v2; http://genetics.bwh.harvard.edu/pph2/, last accessed on October 2018), MutPred (v.1.2; http://mutpred.mutdb.org/, last accessed on October 2018), and SIFT(Sorting Intolerant From Tolerant; http://provean.jcvi.org/protein_batch_submit.php?species=human last accessed on October 2018).

2.7. Statistics

Box plots depicting interquartile ranges (IQRs) of control individuals for MALDI MS and LC–MS data were calculated using Origin (OriginLab, Northampton, MA). Statistical analyses were performed using Microsoft Excel.

3. Results

3.1. Mass spectrometric analysis of free plasma N-Glycans

Forty-three patients from the Rede Sarah de Hospitais de Reabilitação were selected as normal controls according to the criteria presented in the experimental section. The methodology used for glycan release, derivatization and purification, as well as the SIL strategy used for the mass spectrometric evaluation, is detailed in the methodology section and presented as a flow chart in Fig. 1. Briefly, the main adaptation from previous methodologies for N-glycan relative quantification in CDG-II patients [6,7] consists in combining the blood plasma of control individuals as a control pool, followed by derivatization with deuterated iodomethane (I-CD_3). The "heavy" N-glycans from the control pool are used as internal references for each control/patient whose N-glycans have been derivatized with regular iodomethane (I-CH_3), referred to as "light" glycans.

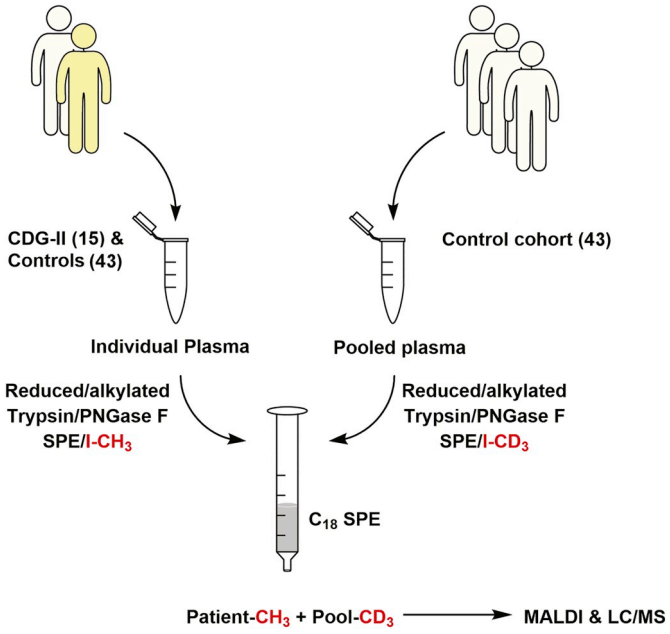

Fig. 1. Flow chart of the stable isotope labelling (SIL) strategy used for N-glycan relative quantification. N-glycans purified from control cohort were permethylated using deuterated iodomethane (I-CD_3) while N-glycans purified from blood serum of each control and CDG-II patients were permethylated independently using regular iodomethane (I-CH_3). Individual and pooled plasma samples were separately submitted to reduction/alkylation, trypsin digestion, PNGase F release of N-glycans and to derivatization. At the final step of purification procedures, permethylated N-glycans from each patient were coeluted with perdeuterated N-glycans purified from control cohort (in a proportion of 2:1 (*v*/v)) across a Sep-Pak C_{18} column. Samples were analyzed by MALDI MS and LC–MS.

MALDI MS analyses of plasma N-glycan samples indicate the prevalence of singly charged Sodium adduct ($[M + Na]^+$) ions, in accordance with the literature [6,7,28]. In addition to the mass of normal permethylated N-glycans in plasma, intense peaks from the heavy derivatized pool sample can be observed (Fig. 2a, ions marked with asterisks). The base peak is given by $[M + Na]^+ = 2792.4$ Da, consistent with HexNAc4Hex5NeuAc2, a disialo biantennary mature N-glycan in its light form. An ion suggesting the heavy isotope of the same glycan, $[M + Na]^+ = 2910.1$ Da, is also detected (Fig. 2a). Relative quantification of the peak $[M + Na]^+ = 2792.4$ Da can be assessed by expressing the area ratio of this ion in relation to its heavy isotope, $[M + Na]^+ = 2910.1$ Da.

The composition of ions whose mass/charge values matched N-glycan structures was confirmed by the acquisition of MS/MS spectra. For such, derivatized plasma N-glycans were analyzed by LC–MS using a reverse-phase C_{18} chromatographic column, and MS/MS spectra were acquired in IDA (Information Dependent Acquisition) mode, following by their submission to an automated identification software aided by manual verification. Using this procedure, 52 ions produced MS/MS spectra with sufficient quality for structural assignment, considering ions from both light and heavy N-glycans (Fig. 2b-c and Supplemental material 2 and 3). Annotated MS/MS spectra of HexNAc4Hex5NeuAc2 (precursor ion at *m/z* $[M + 3Na]^{3+} = 946.1239$) and HexNAc3Hex6-NeuAc1 (precursor ion at *m/z* $[M + 2Na]^{2+} = 1206.5919$) are provided in Fig.s 2b and c as representative examples. The N-glycan ions with insufficient intensity for MS/MS spectra acquisition had their structure inferred from composition alone based on annotations from data banks.

A Total Ion Current Chromatogram (TIC) of the LC–MS analysis of a reference control patient is available in Fig. 3a as an example (dashed line). In general, doubly and triply charged Sodium cations ($[M + 2Na]^{2+}$, and $[M + 3Na]^{3+}$) were detected in LC–MS analysis, although Hydrogen and Potassium adducts were also present (data not shown). Extracted Ion Chromatograms (XICs) relative to N-glycans HexNAc4Hex3Fuc1 (black line), HexNAc4Hex5Fuc1 (red line), HexNAc4Hex5Fuc1NeuAc1 (blue line) and HexNAc4Hex5Fuc1NeuAc2 (green line) are also presented in Fig. 3a, and these evidence insufficient chromatographic separation of isomeric structures. Extracted Ion Chromatograms for $[M + 2Na]^{2+} = 1314.1437$ Da and $[M + 2Na]^{2+} = 1368.4826$ Da, obtained for the light and heavy isotopes of the HexNAc4Hex5Fuc1NeuAc1 glycan of a control individual (Fig. 3b) and a CDG-II patient (Fig. 3c) are provided, along with their corresponding mass spectra (Fig. 3d and e). The area ratio of the aforementioned ions is provided in Fig. 3f.

3.2. Quantification of N-glycans

Quantification methods for plasma N-glycans were developed for both MALDI MS and LC–MS analyses. Thirty-five ions from permethylated glycans were included in the MALDI MS quantification method, based on 5 deuterated glycans (Fig. 2, peaks marked with asterisks). LC–MS analyses allowed the relative quantification of 86 ions based on 23 of their deuterated counterparts. Table 1 lists a selection of glycan structures and their corresponding heavy glycans used for quantification. The glycan composition and mass as a singly charged Sodium adduct are also provided, and structures confirmed by MS/MS experiments are indicated. Given the large number of evaluated structures, a code number was created, and this code is used throughout this manuscript. A full list of the 86 evaluated glycans is provided as supplemental material (Supplemental material 1, Table S1).

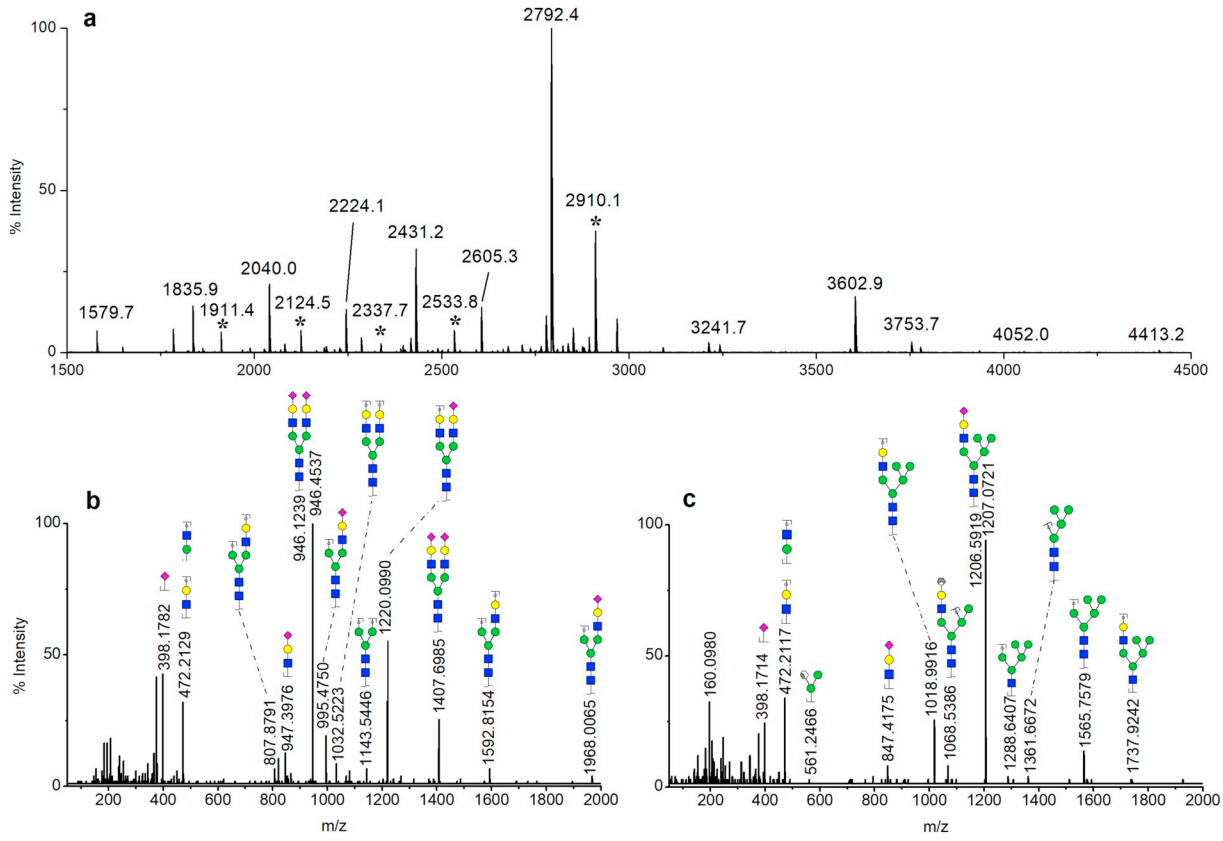

Fig. 2. Mass spectrometry analysis of permethylated glycans. A) MALDI MS acquisition of N-glycans from a control patient. The base peak is given by the N-glycan HexNAc4Hex5NeuAc2 in the permethylated form ($[M + Na]^+ = 2792.4$ Da), followed by ionization of the same N-glycan structure obtained from the control pool derivatized with deuterated iodomethane ($[M + Na]^+ = 2910.1$ Da). Asterisks nominate ions related to deuterated structures from control pool used for N-glycan quantification, namely, $[M + Na]^+ = 1911.4$ Da, $= 2124.5$ Da, $= 2337.7$ Da, 2533.8 Da, and 2910.1 Da. B and C) Assignment of structures matching to the fragment ions of the N-glycan HexNAc4Hex5NeuAc2 (precursor ion at *m/z* $[M + 3Na]^{3+} = 946.1239$) and N-glycan HexNAc3Hex6NeuAc1 (precursor ion at *m/z* $[M + 2Na]^{2+} = 1206.5919$), respectively.

To provide a measure of the dispersion of area ratios of plasma N-glycans in control patients, these were individually evaluated against the pool. Box plots depicting interquartile ranges (IQRs) of the evaluated glycans in control individuals were constructed (Fig. 4a and b). N-glycans showed a wide dispersion in normal individuals. While some glycan species presented narrow distributions around the mean, others, such as glycan number 80 (HexNAc6Hex7NeuAc4), varied up to 12-fold in normal individuals.

A standard additional method was used to investigate the linearity of the area ratios of N-glycans. For such, varying volumes of the heavy isotope pool were mixed with a fixed amount of a reference sample of light glycans, resulting in theoretical area ratios of 4:1; 2:1; 1:1 and 1:1.5, of the light:heavy isotopes, respectively. Samples were analyzed in triplicates and mean area ratios were recorded (Supplemental material 1, Tables S2 and S3). Nine out of the 35 glycan ions evaluated by MALDI MS, and 51 out of 86 in LC–MS, presented a squared correlation coefficient (R^2) higher than or equal to 0.80 for the area ratios versus light:heavy isotope theoretical ratios (Supplemental material 1, Tables S2 and S3). Some ions from glycans present at very low concentrations in normal individuals, such as the hybrid type glycan 40 (HexNAc3Hex6Fuc1NeuAc1) and complex type glycan 70 (HexNAc7Hex8), showed $R^2 \geq 0.95$, in the proposed methodology.

3.2.1. Relative quantification of N-glycans in congenital disorders of glycosylation type II

Fifteen suspected CDG-II patients previously diagnosed by routine transferrin IEF in the Rede Sarah de Hospitais de Reabilitação had their plasma N-glycans evaluated. The N-glycans of 2 siblings diagnosed at the Radboud University Medical Center as ATP6V0A2-CDG with homozygous c.187C > T/p.Arg63* mutations and confirmed at the Sarah Hospital (Supplemental material 4) were analyzed (Fig. 5). The p.Arg63* mutation had been previously observed in other ATP6V0A2-CDG patients and is reported as pathogenic in the ClinVar database. The MALDI MS and LC–MS analyses of N-glycans of sibling 1 are depicted in Fig. 5a and b, respectively, and sibling 2 in Fig. 5c and d. The relative concentration of N-glycans in patients are represented as black dots over red box plots obtained for control individuals, providing a straightforward visual clue for the identification of abnormal glycan concentrations. The structure of N-glycans with relative concentrations above data outliers in the normal population are provided as insets in Fig. 5. Glycans 13 (HexNAc5Hex3Fuc1), 21 (HexNAc5Hex3Fuc1), and 28 (HexNAc5Hex4Fuc1) were increased in both MALDI MS and LC–MS analyses for sibling number 1. Additionally, MALDI MS data pointed to abnormal glycan 19 (HexNAc4Hex4Fuc1), while LC–MS indicated that glycans 5 (HexNAc3Hex3), 15 (HexNAc5Hex3), 20 (HexNAc4Hex5), 26 (HexNAc4Hex4NeuAc1), and 35 (HexNAc4Hex5NeuAc1) were also above the normal range. Analysis of N-glycans of sibling 2 demonstrates that ATP6V0A2-CDG patients can vary significantly even among siblings carrying the same mutation. While MALDI MS did not detect significant alterations from normality in sibling 2, LC–MS pointed to alterations in glycans 5, 15, and 26, which were also altered in sibling 1. Indeed, glycan 15 showed a ~20-fold increase in relation to control individuals in both patients, being this the glycan structure that deviated more significantly from normal levels.

Relative quantification of plasma N-glycans was also performed in a previously diagnosed MAN1B1-CDG patient carrying a p.I428fs*43/

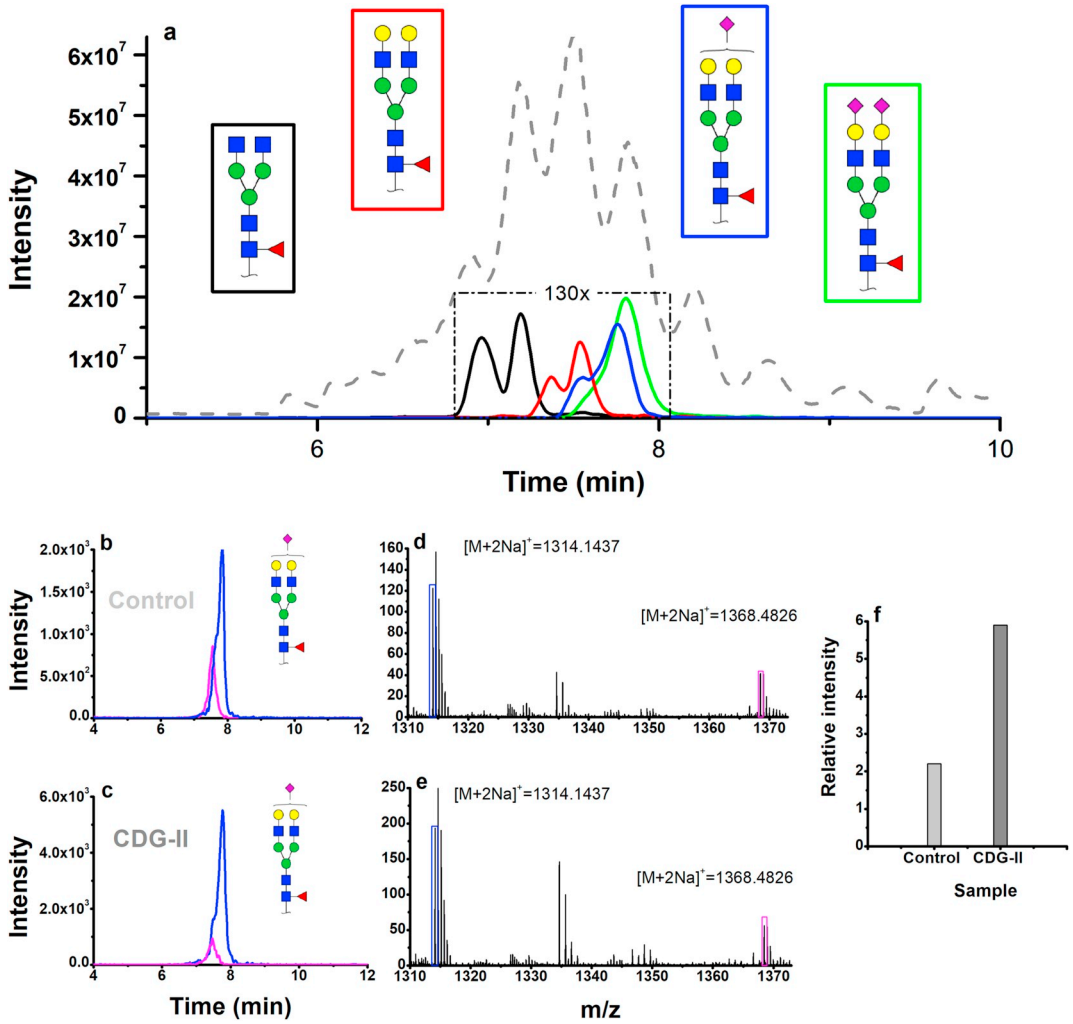

Fig. 3. Analysis of N-glycan structures by LC–MS. A) Total ion current chromatogram (dotted line) and extracted ion chromatogram for N-glycans HexNAc4Hex3Fuc1 (black line), HexNAc4Hex5Fuc1 (red line), HexNAc4Hex5Fuc1NeuAc1 (blue line) and HexNAc4Hex5Fuc1NeuAc2 (green line). Extracted ion chromatogram from the ions $[M + 2Na]^{2+}$ = 1314.1437 Da (blue) and $[M + 2Na]^{2+}$ = 1368.4826 Da (pink) represents light and heavy isotopes of HexNAc4Hex5Fuc1NeuAc1 structure, respectively, isolated from B) control individual and C) CDG-II patient. Corresponding mass spectra from D) control individual and E) CDG-II patient are showed. F) Ratios calculated for areas under the peaks resulted from extracted ion chromatogram for each patient. (For interpretation of the references to colour in this figure legend, the reader is referred to the web version of this article.)

p.S409P mutation [12] (Fig. 6a and b). The glycan 32 (HexNAc3Hex6NeuAc1) was abnormally increased in both MALDI MS and LC–MS analyses, the latter also pointing to glycans 24 (HexNAc3Hex5NeuAc1), 31 (HexNAc3Hex5Fuc1NeuAc1), and 40 (HexNAc3Hex6Fuc1NeuAc1). Glycans 32 and 40 presented 7- and 10-fold increase, respectively, in relation to the mean concentration in normal individuals. These 2 glycans were also abnormally elevated in an undiagnosed patient with an IEF profile suggestive of CDG-II (Fig. 6c and d). The abnormal profile indicative of MAN1B1 was confirmed by gene sequencing, which revealed a c.1607G > T/p.Gly536Val missense mutation (Supplemental material 4), which was not present in variant databases.

4. Discussion

The present work applies a SIL-based strategy to the quantification of plasma N-glycans in CDG-II patients using MALDI MS and LC–MS. The ions detected in MALDI MS analyses of free plasma N-glycans of control individuals derivatized with iodomethane coincide with those extensively reported in the literature [6,7]. Furthermore, ions from deuterated glycans from the control pool were also detected. To expand the number of evaluated ions, LC–MS analyses of mixtures of light and heavy N-glycans were also performed. As anticipated from previous reports [30], poor sample separation of such complex mixtures of glycans was observed by HPLC using a reverse phase chromatographic column. MS/MS spectra were acquired for the detected ions and these corroborate that the detected ions are indeed mixtures of structural isomers. The structures drawn in Table 1 and in the supplemental material are representative of all glycan structural isomers detected in the MS/MS spectra. So, the quantitative relations obtained in the present study may not result from single isomeric species, but rather to mixtures of isobaric molecules. Improvements in the separation methodology, e.g. variations in stationary phase of chromatographic columns, eluents, run times, and temperature [30,31] are currently being evaluated, and these may allow the quantification of individual isomers in the near future.

The quantification of free plasma glycans in CDG-II patients is usually performed by normalizing each ion to the area of all detected glycan compounds, as reported in the literature [7,32,33]. As suggested elsewhere, this approach, although useful, can impart difficulties in the quantification of minor components due to the undue influence of highly concentrated glycan species [34]. The simultaneous analysis of light and heavy molecules, the latter from a pool of control subjects, allowed normalization of areas in a glycan-by-glycan approach, with

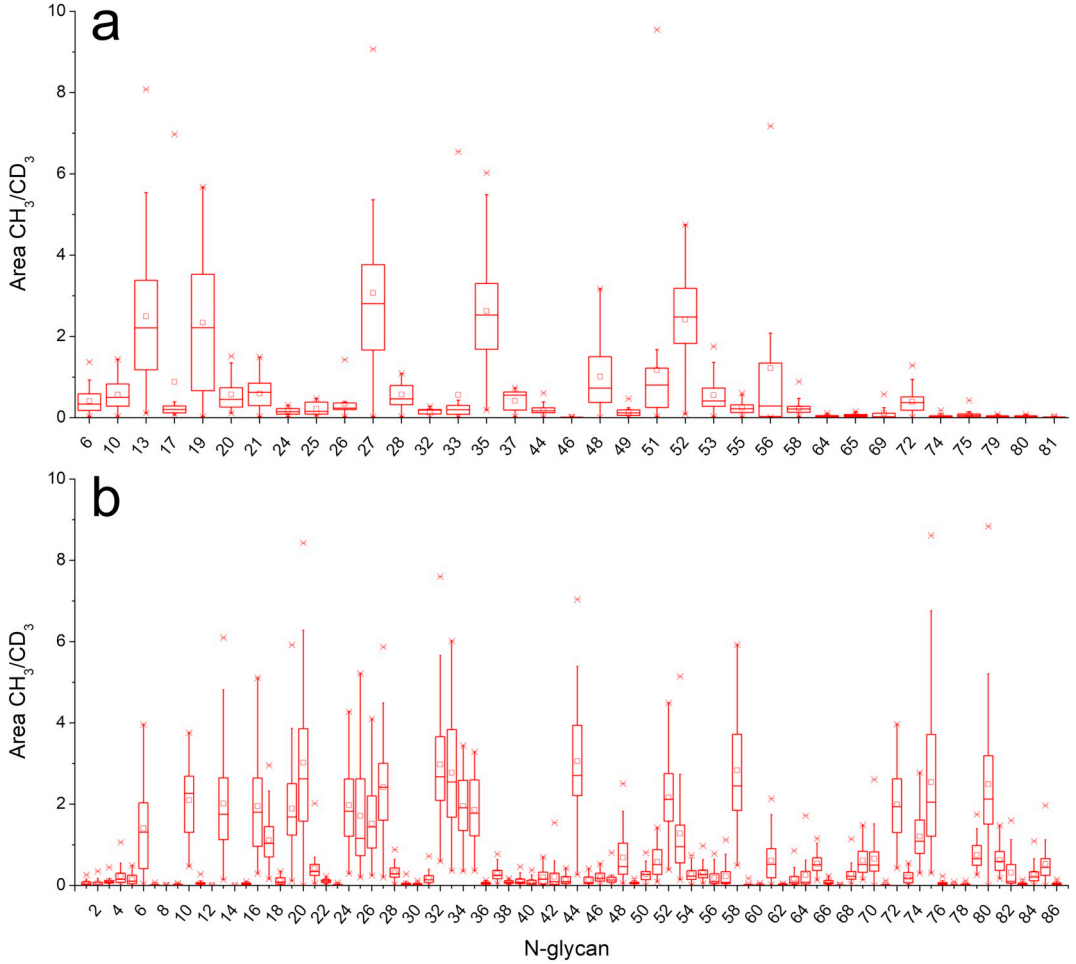

Fig. 4. Box plot of the relative quantification of N-glycan profiles obtained from 43 normal patients performed by A) MALDI and B) LC–MS. Numbers of abscissa represent N-glycan structures listed in Table 1 and Supplemental material 1. The inter-quartile range holds 50% of the data points. The lower and upper whiskers represent the 5th and 95th percentile, respectively, while the median is represented as a straight line, the mean by an open box (□) and data outliers are represented by the ✕ symbol.

estimation of population variance in an individual basis. To illustrate the consequences of this approach, the reference range (95% confidence interval) of GlcNac2Hex9 in the normal population was reported as 0.6–0.7 [32], while using our methodology, the reference range using the same confidence interval was 2.3–3.2. A higher variance may help to identify deviations from normality in this and other less concentrated glycan species. However, practical advantages over other methodologies in the diagnosis of CDG-II must still be verified.

The robustness of the quantification approach described herein, especially for LC–MS analyses, is another important aspect. The linearity of response in glycan quantification was investigated by comparing the theoretical versus actual area ratios of light and heavy glycans. Considering that the theoretical ratio of heavy glycans to light glycans in normal patients is 1:2, it is expected that those quantified by their own heavy counterpart display an average area ratio of 2. This is indeed observed for 22 different structures in the LC–MS method, as exemplified for glycan 34 (HexNAc4Hex5Fuc1NeuAc1), with an average area ratio of 1.95 ± 0.81. This observation is consistent with previous publications that state that equimolar mixtures of light- and heavy-derivatized glycans generate peaks of the same intensity following mass spectrometric evaluation [25]. The low linearity of response of some glycan species might be related to their low concentration in unaffected individuals, in contrast to their accumulation in some CDG-II subtypes. It is indeed challenging to quantify such large number of structures in complex samples that undergo extensive sample preparation and may be subject to matrix effects [35].

Our quantification method was applied to fifteen putative CDG-II patients diagnosed by standard Transferrin IEF. Two ATP6V0A2-CDG patients carrying a p.Arg63* mutation were evaluated, and these were shown to accumulate hypogalactosylated and hyposialylated structures, in agreement with a previous paper [6], which reports an increase in complex biantennary truncated structures lacking galactose and sialic acid for this CDG-II subtype. The glycan 15 (HexNAc5Hex3) was the one that deviated more significantly from average concentration in our patients. Due to its consistency, we suggest it should be meticulously evaluated as a putative marker in other individuals of the same CDG-II subtype. Interestingly, MALDI MS analysis did not produce a significant signal for this ion, $[M + Na]^+ = 1907.0$ Da, which indicates that this is a minor component usually neglected in MALDI MS measurements. ATP6V0A2-CDG is caused by impaired Golgi trafficking, as are COGx-, TMEM165-, and SLC35A2-CDG [3]. All these subtypes produce similar spectra [8] and so far, no mass spectrometry methodology was able to reliably distinguish between them. We speculate that a glycan-by-glycan approach to the quantification of free plasma glycans might produce specific markers for different Golgi trafficking disorders.

A patient with a previously diagnosed MAN1B1 homozygous pathogenic mutation was also evaluated. MAN1B1-CDG is caused by mutations in the enzyme α(1,2)-mannosidase, which catalyzes the removal of the terminal mannose residue from the middle branch of the glycan Man9GlcNAc2 [12,13,36]. Previous reports indicate that the peaks *m/z* 2186, 2360, 2390 and 2564, corresponding to glycan numbers 24 (HexNAc3Hex5NeuAc1), 31 HexNac3HexFuc1NeuAc1), 32

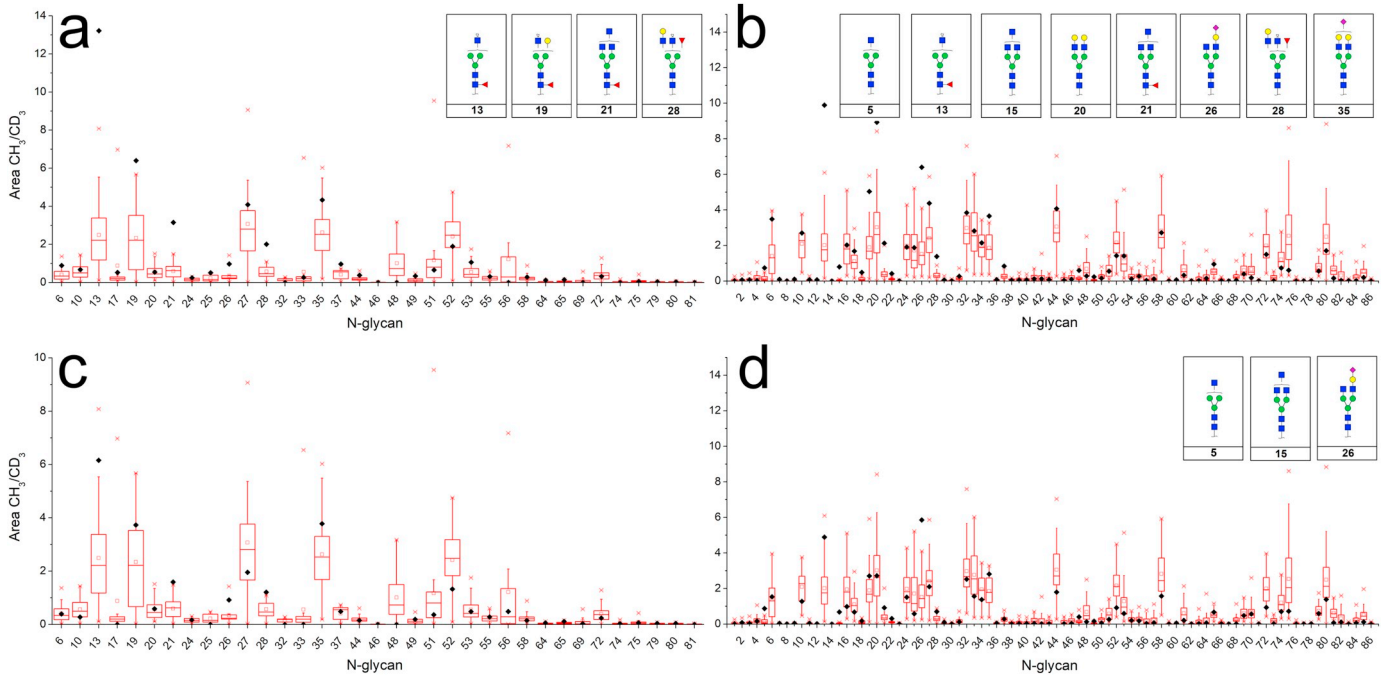

Fig. 5. Relative quantification of N-glycans of two siblings diagnosed as ATP6V0A2-CDG carrying p.Arg63* mutations performed by A) and C) MALDI and B and D) LC–MS in relation to normal controls. Results for sibling 1 (A and B) and sibling 2 (C and D) were plotted as black diamonds against the box plot obtained from controls. Structures presenting relative concentrations above data outliers in the normal population are indicated in insets. Numbers of abscissa represent N-glycan structures listed in Table 1 and Supplemental material 1. The inter-quartile range holds 50% of the data points. The lower and upper whiskers represent the 5th and 95th percentile, respectively, while the median is represented as a straight line, the mean by an open box (□) and data outliers are represented by the ✱ symbol.

(HexNac3Hex6NeuAc1) and 40 (HexNAc3Hex6Fuc1NeuAc1) in our reference system, present in almost undetectable concentrations in normal individuals, are characteristic of this particular CDG-II subtype [8]. These reporter ions for MAN1B1-CDG were also detected in an undiagnosed patient, leading to a putative diagnosis, which was later confirmed by gene sequencing. The MAN1B1 gene variant p.Gly536Val

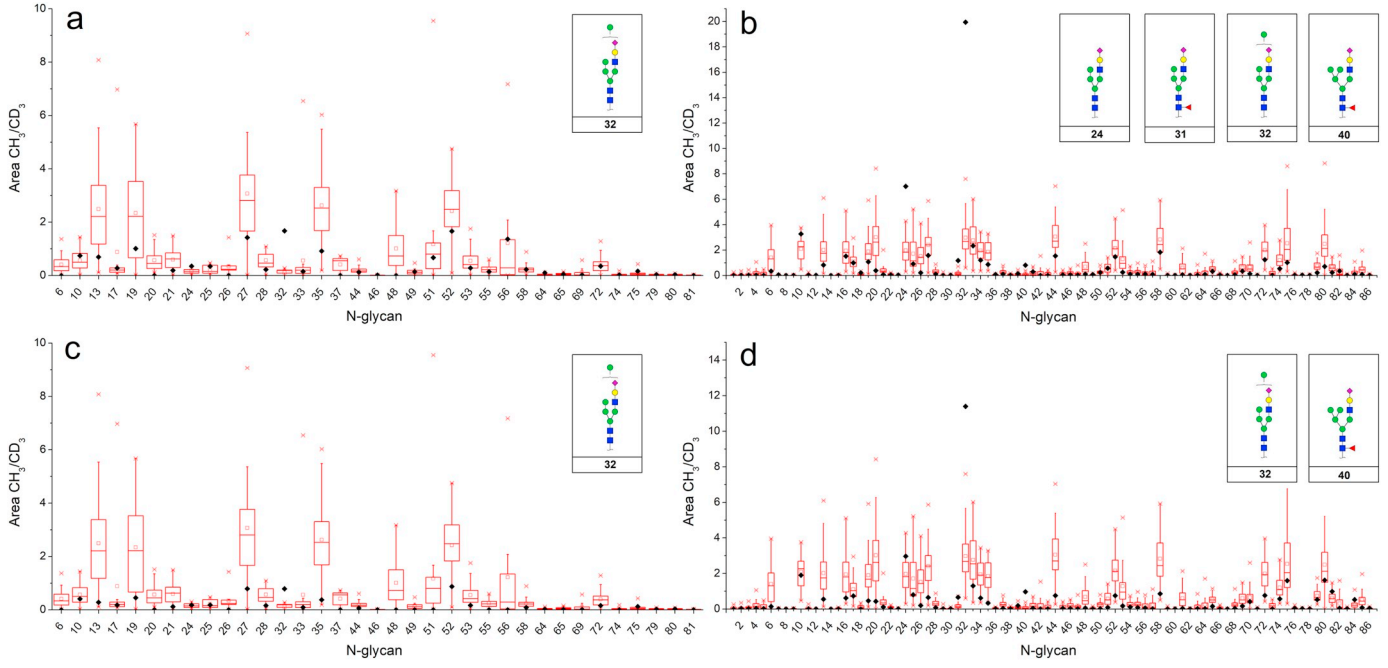

Fig. 6. Serum N-glycan profile obtained from the analysis of a MAN1B1-CDG patient performed by A) MALDI and B) LC–MS. The C) MALDI and D) LC–MS glycan profile of another MAN1B1-CDG patient carrying a novel p.Gly536Val mutation is also presented, demonstrating the accumulation of structures 32 and 40. Results were plotted as black diamonds against red box plots obtained for controls. Structures presenting relative concentrations above data outliers in the normal population are indicated in insets. Numbers of abscissa represent N-glycan structures listed in Table 1 and Supplemental material 1. The inter-quartile range holds 50% of the data points. The lower and upper whiskers represent the 5th and 95th percentile, respectively, while the median is represented as a straight line, the mean by an open box (□) and data outliers are represented by the ✱ symbol. (For interpretation of the references to colour in this figure legend, the reader is referred to the web version of this article.)

is not reported in databases. However, bioinformatics predictions using PolyPhen2, SIFT and MutPred are concordant for a pathogenic role for this mutation. Further investigations on the pathogenicity of this variant will be conducted in later publications by our group.

It is also relevant to discuss the potential of MALDI MS and LC–MS in providing information for the diagnosis of CDG-II subtypes. Although it was demonstrated that relative quantification of glycans by MALDI MS is consistent with LC–MS, providing similar information with quantitative value, corroborating the literature [37], MALDI MS analyses are overall less informative. While valuable as a preliminary screening approach due to its easiness in terms of sample preparation and mass spectra interpretation, MALDI MS signal suppression and mass accuracy restrictions limit the number of glycans ions to be identified unambiguously. Yet, the LC–MS based quantification method proposed also needs to be improved aiming a better separation of isobaric glycans, increasing the number of identified structures and the reliability of the methodology. Furthermore, questions inherent to the efficiency of the method as a preliminary screening tool, as well as the probability of false negative and false positive results, can be answered only after the analysis of an extended set of CDG-II patients with molecular diagnostics.

The plasma N-glycans of the 11 remaining suspected CDG-II patients were also evaluated. Glycan profiles of 4 of these patients were indicative of Golgi trafficking disorders, with increased concentration of truncated glycan species (data not shown). Considering the current unavailability of molecular diagnostics for these patients, a future study concerning both clinical and biochemical aspects of their diseases will be conducted. It is expected that once gene sequencing becomes available, the methodology proposed herein might assist the recognition of diagnostic profiles for novel CDG-II subtypes, especially those related to Golgi trafficking disorders.

Acknowledgement

The authors wish to express their gratitude to Rede Sarah de Hospitais, Universidade de Brasília and Empresa Brasileira de Pesquisa Agropecuária. This study was financed in part by the Coordenação de Aperfeiçoamento de Pessoal de Nível Superior - Brasil (CAPES) - Finance Code 001.

Appendix A. Supplementary data

Supplementary data to this article can be found online at https://doi.org/10.1016/j.cca.2019.02.013.

References

[1] C.B. Lebrilla, H.J. An, The prospects of glycanbiomarkers for the diagnosis of diseases, Mol. BioSyst. 5 (2009) 17–20, https://doi.org/10.1039/B811781K.
[2] A. Varki, R.D. Cummings, J.D. Esko, H.H. Freeze, P. Stanley, C.R. Bertozzi, G.W. Hart, M.E. Etzler, Essentials of Glycobiology, Cold Spring Harbor Laboratory Press, 2009, http://www.ncbi.nlm.nih.gov/pubmed/20301239 (accessed October 2, 2017).
[3] K. Scott, T. Gadomski, T. Kozicz, E. Morava, Congenital disorders of glycosylation: new defects and still counting, J. Inherit. Metab. Dis. 37 (2014) 609–617, https://doi.org/10.1007/s10545-014-9720-9.
[4] C.R. Ferreira, R. Altassan, D. Marques-Da-Silva, R. Francisco, J. Jaeken, E. Morava, Recognizable phenotypes in CDG, J. Inherit. Metab. Dis. (2018), https://doi.org/10.1007/s10545-018-0156-5.
[5] A.G. Woods, C.W. Woods, T.M. Snow, Congenital disorders of glycosylation, Adv. Neonatal Care. 12 (2012) 90–95, https://doi.org/10.1097/ANC.0b013e318241cb20.
[6] M. Guillard, E. Morava, F.L. van Delft, R. Hague, C. Korner, M. Adamowicz, R.A. Wevers, D.J. Lefeber, Plasma N-glycan profiling by mass spectrometry for congenital disorders of glycosylation type II, Clin. Chem. 57 (2011) 593–602, https://doi.org/10.1373/clinchem.2010.153635.
[7] B. Xia, W. Zhang, X. Li, R. Jiang, T. Harper, R. Liu, R.D. Cummings, M. He, Serum N-glycan and O-glycan analysis by mass spectrometry for diagnosis of congenital disorders of glycosylation, Anal. Biochem. 442 (2013) 178–185, https://doi.org/10.1016/j.ab.2013.07.037.
[8] N. Abu Bakar, D.J. Lefeber, M. van Scherpenzeel, Clinical glycomics for the diagnosis of congenital disorders of glycosylation, J. Inherit. Metab. Dis. (2018), https://doi.org/10.1007/s10545-018-0144-9.
[9] P. Witters, D. Cassiman, E. Morava, P. Witters, D. Cassiman, E. Morava, Nutritional therapies in congenital disorders of glycosylation (CDG), Nutrients 9 (2017) 1222 (doi:10.3390/nu9111222).
[10] M. Van Scherpenzeel, G. Steenbergen, E. Morava, R.A. Wevers, D.J. Lefeber, High-resolution mass spectrometry glycoprofiling of intact transferrin for diagnosis and subtype identification in the congenital disorders of glycosylation, Transl. Res. 166 (2015) 639–649, https://doi.org/10.1016/j.trsl.2015.07.005.
[11] W. Zhang, P.M. James, B.G. Ng, X. Li, B. Xia, J. Rong, G. Asif, K. Raymond, M.A. Jones, M. Hegde, T. Ju, R.D. Cummings, K. Clarkson, T. Wood, C.F. Boerkoel, H.H. Freeze, M. He, A novel N-Tetrasaccharide in patients with congenital disorders of glycosylation, including asparagine-linked glycosylation protein 1, Phosphomannomutase 2, and mannose phosphate Isomerase deficiencies, Clin. Chem. 62 (2016) 208–217, https://doi.org/10.1373/clinchem.2015.243279.
[12] M. Van Scherpenzeel, S. Timal, D. Rymen, A. Hoischen, M. Wuhrer, A. Hipgrave-Ederveen, S. Grunewald, R. Peanne, A. Saada, S. Edvardson, S. Grønborg, G. Ruijter, A. Kattentidt-Mouravieva, J.M. Brum, M.L. Freckmann, S. Tomkins, A. Jalan, D. Prochazkova, N. Ondruskova, H. Hansikova, M.A. Willemsen, P.J. Hensbergen, G. Matthijs, R.A. Wevers, J.A. Veltman, E. Morava, D.J. Lefeber, Diagnostic serum glycosylation profile in patients with intellectual disability as a result of MAN1B1 deficiency, Brain 137 (2014) 1030–1038, https://doi.org/10.1093/brain/awu019.
[13] D. Rymen, R. Peanne, M.B. Millón, V. Race, L. Sturiale, D. Garozzo, P. Mills, P. Clayton, C.G. Asteggiano, D. Quelhas, A. Cansu, E. Martins, M.-C. Nassogne, M. Gonçalves-Rocha, H. Topaloglu, J. Jaeken, F. Foulquier, G. Matthijs, MAN1B1 deficiency: an unexpected CDG-II, PLoS Genet. 9 (2013) e1003989, , https://doi.org/10.1371/journal.pgen.1003989.
[14] E. Reynders, F. Foulquier, E. Leão Teles, D. Quelhas, W. Morelle, C. Rabouille, W. Annaert, G. Matthijs, Golgi function and dysfunction in the first COG4-deficient CDG type II patient, Hum. Mol. Genet. 18 (2009) 3244–3256, https://doi.org/10.1093/hmg/ddp262.
[15] C.W. Fung, G. Matthijs, L. Sturiale, D. Garozzo, K.Y. Wong, R. Wong, V. Wong, J. Jaeken, COG5-CDG with a mild Neurohepatic presentation, JIMD Rep. 3 (2012) 67–70, https://doi.org/10.1007/8904_2011_61.
[16] A. Palmigiano, R.O. Bua, R. Barone, D. Rymen, L. Régal, N. Deconinck, C. Dionisi-Vici, C.-W. Fung, D. Garozzo, J. Jaeken, L. Sturiale, MALDI-MS profiling of serum O-glycosylation and N-glycosylation in COG5-CDG, J. Mass Spectrom. 52 (2017) 372–377, https://doi.org/10.1002/jms.3936.
[17] F. Foulquier, M. Amyere, J. Jaeken, R. Zeevaert, E. Schollen, V. Race, R. Bammens, W. Morelle, C. Rosnoblet, D. Legrand, D. Demaegd, N. Buist, D. Cheillan, N. Guffon, P. Morsomme, W. Annaert, H.H. Freeze, E. Van Schaftingen, M. Vikkula, G. Matthijs, TMEM165 deficiency causes a congenital disorder of glycosylation, Am. J. Hum. Genet. 91 (2012) 15–26, https://doi.org/10.1016/j.ajhg.2012.05.002.
[18] J.C. Jansen, S. Timal, M. van Scherpenzeel, H. Michelakakis, D. Vicogne, A. Ashikov, M. Moraitou, A. Hoischen, K. Huijben, G. Steenbergen, M.A.W. van den Boogert, F. Porta, P.L. Calvo, M. Mavrikou, G. Cenacchi, G. van den Bogaart, J. Salomon, A.G. Holleboom, R.J. Rodenburg, J.P.H. Drenth, M.A. Huynen, R.A. Wevers, E. Morava, F. Foulquier, J.A. Veltman, D.J. Lefeber, TMEM199 deficiency is a disorder of Golgi homeostasis characterized by elevated aminotransferases, alkaline phosphatase, and cholesterol and abnormal glycosylation, Am. J. Hum. Genet. 98 (2016) 322–330, https://doi.org/10.1016/j.ajhg.2015.12.011.
[19] J.C. Jansen, S. Cirak, M. van Scherpenzeel, S. Timal, J. Reunert, S. Rust, B. Pérez, D. Vicogne, P. Krawitz, Y. Wada, A. Ashikov, C. Pérez-Cerdá, C. Medrano, A. Arnoldy, A. Hoischen, K. Huijben, G. Steenbergen, D. Quelhas, L. Diogo, D. Rymen, J. Jaeken, N. Guffon, D. Cheillan, L.P. van den Heuvel, Y. Maeda, O. Kaiser, U. Schara, P. Gerner, M.A.W. van den Boogert, A.G. Holleboom, M.-C. Nassogne, E. Sokal, J. Salomon, G. van den Bogaart, J.P.H. Drenth, M.A. Huynen, J.A. Veltman, R.A. Wevers, E. Morava, G. Matthijs, F. Foulquier, T. Marquardt, D.J. Lefeber, CCDC115 deficiency causes a disorder of Golgi homeostasis with abnormal protein glycosylation, Am. J. Hum. Genet. 98 (2016) 310–321, https://doi.org/10.1016/j.ajhg.2015.12.010.
[20] E.J.R. Jansen, S. Timal, M. Ryan, A. Ashikov, M. van Scherpenzeel, L.A. Graham, H. Mandel, A. Hoischen, T.C. Iancu, K. Raymond, G. Steenbergen, C. Gilissen, K. Huijben, N.H.M. van Bakel, Y. Maeda, R.J. Rodenburg, M. Adamowicz, E. Crushell, H. Koenen, D. Adams, J. Vodopiutz, S. Greber-Platzer, T. Müller, G. Dueckers, E. Morava, J. Sykut-Cegielska, G.J.M. Martens, R.A. Wevers, T. Niehues, M.A. Huynen, J.A. Veltman, T.H. Stevens, D.J. Lefeber, ATP6AP1 deficiency causes an immunodeficiency with hepatopathy, cognitive impairment and abnormal protein glycosylation, Nat. Commun. 7 (2016) 11600, , https://doi.org/10.1038/ncomms11600.
[21] M.A. Rujano, M. Cannata Serio, G. Panasyuk, R. Péanne, J. Reunert, D. Rymen, V. Hauser, J.H. Park, P. Freisinger, E. Souche, M.C. Guida, E.M. Maier, Y. Wada, S. Jäger, N.J. Krogan, O. Kretz, S. Nobre, P. Garcia, D. Quelhas, T.D. Bird, W.H. Raskind, M. Schwake, S. Duvet, F. Foulquier, G. Matthijs, T. Marquardt, M. Simons, Mutations in the X-linked ATP6AP2 cause a glycosylation disorder with autophagic defects, J. Exp. Med. 214 (2017) 3707–3729, https://doi.org/10.1084/jem.20170453.
[22] C. Grunwald-Gruber, A. Thader, D. Maresch, T. Dalik, F. Altmann, Determination of true ratios of different N-glycans structures in electrospray ionization mass spectrometry, Anal. Bioanal. Chem. 409 (10) (2017) 2519–2530, https://doi.org/10.1007/s00216-017-0235-8.
[23] E.S.X. Moh, M. Thaysen-Andersen, N.H. Packer, Relative versus absolute quantitation in disease glycomics, Proteomics: Clin. Appl. 9 (2015) 368–382, https://doi.org/10.1002/prca.201400184.
[24] Y. Mechref, Y. Hu, J.L. Desantos-Garcia, A. Hussein, H. Tang, Quantitative

glycomics strategies, Mol. Cell. Proteomics. 12 (2013) 874–884, https://doi.org/10.1074/mcp.R112.026310.
[25] G. Alvarez-Manilla, N.L. Warren, T. Abney, J. Atwood, P. Azadi, W.S. York, M. Pierce, R. Orlando, Tools for glycomics: relative quantitation of glycans by isotopic permethylation using 13CH3I, Glycobiology 17 (2007) 677–687 (doi:10.1093/glycob/cwm033).
[26] L.R. Ruhaak, G. Zauner, C. Huhn, C. Bruggink, A.M. Deelder, M. Wuhrer, Glycan labeling strategies and their use in identification and quantification, Anal. Bioanal. Chem. 397 (2010) 3457–3481, https://doi.org/10.1007/s00216-010-3532-z.
[27] C. Grünwald-Gruber, A. Thader, D. Maresch, T. Dalik, F. Altmann, Determination of true ratios of different N-glycan structures in electrospray ionization mass spectrometry, Anal. Bioanal. Chem. 409 (2017) 2519–2530, https://doi.org/10.1007/s00216-017-0235-8.
[28] W. Morelle, J.-C. Michalski, Analysis of protein glycosylation by mass spectrometry, Nat. Protoc. 2 (2007) 1585–1602, https://doi.org/10.1038/nprot.2007.227.
[29] A. Ceroni, K. Maass, H. Geyer, R. Geyer, A. Dell, S.M. Haslam, GlycoWorkbench: a tool for the computer-assisted annotation of mass spectra of Glycans †, J. Proteome Res. 7 (2008) 1650–1659, https://doi.org/10.1021/pr7008252.
[30] G.C.M. Vreeker, M. Wuhrer, Reversed-phase separation methods for glycan analysis, Anal. Bioanal. Chem. 409 (2017) 359–378, https://doi.org/10.1007/s00216-016-0073-0.
[31] S. Zhou, Y. Hu, Y. Mechref, High-temperature LC–MS/MS of permethylated glycans derived from glycoproteins, Electrophoresis 37 (2016) 1506–1513, https://doi.org/10.1002/elps.201500568.
[32] A. Ashikov, N. Abu Bakar, X.-Y. Wen, M. Niemeijer, G. Rodrigues Pinto Osorio, K. Brand-Arzamendi, L. Hasadsri, H. Hansikova, K. Raymond, D. Vicogne, N. Ondruskova, M.E.H. Simon, R. Pfundt, S. Timal, R. Beumers, C. Biot, R. Smeets, M. Kersten, K. Huijben, P.T.A. Linders, G. van den Bogaart, S.A.F.T. van Hijum, R. Rodenburg, L.P. van den Heuvel, F. van Spronsen, T. Honzik, F. Foulquier, M. van Scherpenzeel, D.J. Lefeber, W. Mirjam, B. Han, M. Helen, M. Helen, van H. Peter, van de K. Jiddeke, M. Diego, M. Lars, B.H. Katja, H. Jozef, A. Majid, C. Kevin, te W.N. Johann, C. Kevin, T.W.N. Johann, Integrating glycomics and genomics uncovers SLC10A7 as essential factor for bone mineralization by regulating post-Golgi protein transport and glycosylation, Hum. Mol. Genet. 27 (2018) 3029–3045, https://doi.org/10.1093/hmg/ddy213.
[33] E. Morava, F.L. Van Delft, R. Hague, C. Körner, M. Adamowicz, R.A. Wevers, D.J. Lefeber, Plasma N-glycan profiling by mass spectrometry for congenital disorders of glycosylation type II methods, Clin. Chem. (2011) 593–602, https://doi.org/10.1373/clinchem.2010.153635.
[34] N. Mehta, M. Porterfield, W.B. Struwe, C. Heiss, P. Azadi, P.M. Rudd, M. Tiemeyer, K. Aoki, Mass spectrometric quantification of N-linked Glycans by reference to exogenous standards, J. Proteome Res. 15 (2016) 2969–2980, https://doi.org/10.1021/acs.jproteome.6b00132.
[35] P.J. Taylor, Matrix effects: the Achilles heel of quantitative high-performance liquid chromatography–electrospray–tandem mass spectrometry, Clin. Biochem. 38 (2005) 328–334, https://doi.org/10.1016/J.CLINBIOCHEM.2004.11.007.
[36] R. Saldova, H. Stöckmann, R. O'Flaherty, D.J. Lefeber, J. Jaeken, P.M. Rudd, N-glycosylation of serum IgG and Total glycoproteins in MAN1B1 deficiency, J. Proteome Res. 14 (2015) 4402–4412, https://doi.org/10.1021/acs.jproteome.5b00709.
[37] Y. Wada, P. Azadi, C.E. Costello, A. Dell, R.A. Dwek, H. Geyer, R. Geyer, K. Kakehi, N.G. Karlsson, K. Kato, N. Kawasaki, K.-H. Khoo, S. Kim, A. Kondo, E. Lattova, Y. Mechref, E. Miyoshi, K. Nakamura, H. Narimatsu, M.V. Novotny, N.H. Packer, H. Perreault, J. Peter-Katalinić, G. Pohlentz, V.N. Reinhold, P.M. Rudd, A. Suzuki, N. Taniguchi, Comparison of the methods for profiling glycoprotein glycans—HUPO human disease Glycomics/proteome initiative multi-institutional study, Glycobiology 17 (2007) 411–422 (doi:10.1093/glycob/cwl086).